Revisiting the Methyl Iodide Oxidative Addition to Rhodium Complexes: A DFT Study of the Activation Parameters

Marta Feliz,[†] Zoraida Freixa,[†] Piet W. N. M. van Leeuwen,[†,§] and Carles Bo*[,†,‡]

Institute of Chemical Research of Catalonia (ICIQ), Avgda. Països Catalans 16, 43007 Tarragona, Spain, Departament de Química Física i Inorgànica, Universitat Rovira i Virgili, Avgda. Marcel.lí Domingo s/n, 43007 Tarragona, Spain, and Van't Hoff Institute for Molecular Sciences, University of Amsterdam, Nieuwe Achtergracht 166, 1018WV Amsterdam, The Netherlands

Received July 2, 2005

Oxidative addition of methyl iodide to rhodium complexes, the first and rate-determining step in the rhodium-catalyzed methanol carbonylation process, has been studied computationally by means of DFT calculations including solvent effects. Monsanto's catalyst *cis*-$[Rh(CO)_2I_2]^-$, Cole−Hamilton's *trans*-$[Rh(PEt_3)_2(CO)I]$, and Freixa's new dirhodium $[Rh_2(\mu\text{-}Cl)_2(SPAN\text{-}PPh_2)(CO)_2]$ complexes were considered. Transition state structures determined in this study confirm the S_N2 character of the reaction, i.e., the nucleophilic attack by the rhodium complex on MeI. The transition states show a linear arrangement of the $I-CH_3-Rh$ moiety. The DFT level of calculation and solvent effects were shown to be crucial in the determination of TS structures. Thermochemical parameters computed in this study were in excellent agreement with experimental kinetic data.

Introduction

Methanol carbonylation to produce acetic acid is one of the most prominent industrial applications of homogeneous catalysis.[1] The original rhodium/iodide process was initiated in 1966 at the Monsanto laboratories.[2,3] The technology ownership was acquired by BP Chemicals in 1986, where it was further developed[4] and licensed over the world. The harsh conditions of the Monsanto process have driven the researchers to the synthesis of new rhodium complexes bearing electron-donating ligands,[5] as these might facilitate the oxidative addition of methyl iodide; whether these systems will provide stable catalyst systems in the long term remains to be studied. Phosphine ligands generated much interest, and several complexes were synthesized and tested as catalysts. The catalytic performance of monophosphines, PEt_3,[6] diphosphines, $PPh_2\text{-}CH_2\text{-}CH_2\text{-}PPh_2$ (dppe),[7] and mixed bidentate ligands $PPh_2\text{-}CH_2\text{-}P(O)Ph_2$ (dppmo),[8] $PPh_2\text{-}(CH_2)_2\text{-}P(O)Ph_2$ (dppeo),[9] $PPh_2\text{-}CH_2\text{-}P(S)Ph_2$(dppms),[10,11] S,P-$SC_2B_{10}H_{10}PPh_2$ ($Cab^{P,S}$),[12] and $PPh_2\text{-}CH_2\text{-}P(NPh)Ph_2$ (dppmn)[13] was similar or better than the Monsanto process. Electronically unsymmetrical diphosphine complexes are also active and selective catalysts in industrially significant conditions.[14] New nitrogen donor ligands, such as the macrocycle dimeric species reported by Süss-Fink et al.,[15] catalyzed the iodide-promoted carbonylation of methanol with higher activity than that of the classical catalyst. The anionic bis(imino)carbazolide ligand reported recently by Haynes et al.[16] is the most active system for methyl iodide oxidative addition, the first and rate-determining step in the catalytic cycle (Scheme 1).[17] Although the first report on the reactivity of dimeric rhodium species with methyl iodide was reported a long time ago,[18] very recently, rhodium dimers stabilized by new *trans*-chelating diphosphine ligands showed high activity. It was proposed[5,15] that rhodium dimers could participate as intermediates in the process. Indeed, the fastest phosphine-based catalyst reported until now is the bimetallic *trans* diphosphine compound $[Rh_2(\mu\text{-}Cl)_2$-

* To whom correspondence should be addressed. E-mail: cbo@iciq.es.
† ICIQ.
‡ Universitat Rovira i Virgili.
§ University of Amsterdam.

(1) (a) Gauss, M.; Seidel, A.; Torrence, P.; Heymans, P. *Applied Homogeneous Catalysis with Organometallic Compunds*; Cornils, B., Herrmann, W. A., Eds.; VCH: New York, 1996. (b) Howard, M. J.; Jones, M. D.; Roberts, M. S.; Taylor, S. A. *Catal. Today* **1993**, *18*, 325.
(2) Forster, D. *J. Am. Chem. Soc.* **1976**, *98*, 846.
(3) Forster, D. *Adv. Organomet. Chem.* **1979**, *17*, 255.
(4) Jones, J. J. *Platinum Met. Rev.* **2000**, *44*, 94.
(5) Thomas, C. M.; Süss-Fink, G. *Coord. Chem. Rev.* **2003**, *243*, 125.
(6) (a) Rankin, J.; Poole, A. D.; Benyei, A. C.; Cole-Hamilton, D. J. *Chem. Commun.* **1997**, 1835. (b) Rankin, J.; Benyei, A. C.; Poole, A. D.; Cole-Hamilton, D. J. *J. Chem. Soc., Dalton Trans.* **1999**, 3771.
(7) Moloy, K. G.; Wegman, R. W. *Organometallics* **1989**, *8*, 2889.
(8) Wegman, R. W. *Chem. Abstr.* **1986**, *105*, 78526g.
(9) Wegman, R. W.; Abutjoglou, A. G.; Harrison, A. M. *J. Chem. Soc., Chem. Commun.* **1987**, 1891.
(10) Baker, M. J.; Giles, M. G.; Orpen, A. G.; Taylor, M. J.; Watt, R. J. *J. Chem. Soc., Chem. Commun.* **1995**, 197.
(11) Gonsalvi, L.; Adams, H.; Sunley, G. J.; Ditzel, E.; Haynes, A. *J. Am. Chem. Soc.* **1999**, *121*, 11233.
(12) Lee, H.-S.; Bae, J.-Y.; Kim, D.-H.; Kim, H. S.; Kim, S.-J.; Cho, S.; Ko, J.; Kang, S. O. *Organometallics* **2002**, *21*, 210−219.
(13) Katti, K. V.; Santarsiero, B. D.; Pinkerton, A. A.; Cavell, R. G. *Inorg. Chem.* **1993**, *32*, 5919.
(14) Carraz, C. A.; Ditzel, E. J.; Orpen, A. G.; Ellis, D. D.; Pringle, P. G.; Sunley, G. J. *Chem. Commun.* **2000**, 1277−1278.
(15) Thomas, C. M.; Neels, A.; Stoeckli-Evans, H.; Süss-Fink, G. *Eur. J. Inorg. Chem.* **2001**, 3005.
(16) Gaunt, J. A.; Gibson, V. C.; Haynes, A.; Spitzmesser, S. K.; White, A. J. P.; Williams, D. J. *Organometallics* **2004**, *23*, 1015.
(17) Haynes, A.; Mailis, P. M.; Stanbridge, I. A.; Haak, S.; Pearson, J. M.; Adams, H.; Bailey, N. A. *Inorg. Chim. Acta* **2004**, *357*, 3027.
(18) Doyle, M. J.; Mayanza, A.; Bonnet, J.-J.; Kalck, P.; Poilblanc, R. J. *J. Organomet. Chem.* **1978**, *146*, 293.

10.1021/om050554g CCC: $30.25
Publication on Web 09/27/2005

Scheme 1

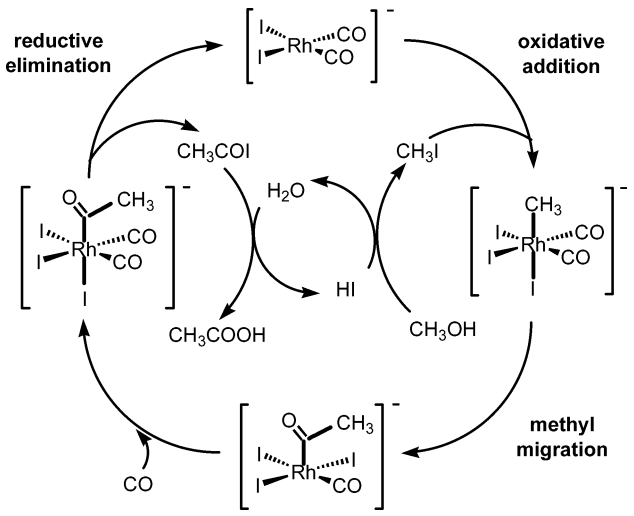

(SPANphos)$(CO)_2$] synthesized by Freixa et al.,[19] which showed unprecedented activity in the methanol carbonylation process. It is worth noting that the activation enthalpy measured for the oxidative addition of MeI in that system is below 10 kcal·mol^{-1}.

The importance of the MeI oxidative addition is well established. It is generally considered to be rate determining[6,20] and to proceed in two steps: S_N2 attack by the Rh(I) complex on MeI followed by iodide coordination to Rh(III). However, theoretical characterization of the mechanism of this fundamental step is still a matter of debate. Despite the great relevance of the process in homogeneous catalysis, accurate computational studies are still scarce due to the inherent complexity of the system. The existence of negatively charged and neutral species along the reaction mechanism and ionic ligand exchange processes pose severe difficulties to gas-phase quantum chemistry methods. Solvent effects become crucial, for instance, in stabilizing the iodide leaving group, which otherwise is a highly unstable species in the gas phase. In a pioneering study on the Monsanto process, Griffin et al.[20] determined the geometry of two TS structures at the Hartree−Fock (HF) level and performed single-point Møller−Plesset (MP2) energy evaluation in the gas phase. In the S_N2-like transition state, MeI approaches $[Rh(CO)_2I_2]^-$ along the axis perpendicular to the plane, the methyl group adopts a five-coordinated trigonal bipyramid structure, and the I−CH_3−Rh angle deviates slightly from linearity (Figure 1a). In the second TS structure, the I−CH_3−Rh angle is bent toward the CO ligands (Figure 1b). The former was found the most stable, thus confirming, for the first time, the S_N2 character of the MeI oxidative addition. However, the energy barrier was overestimated at the HF and MP2 levels. Later, Ziegler et al. studied the migratory CO insertion step,[21] and almost simultaneously, Ivanova et al.[22] and Kinnunen et al.[23−25] reported DFT studies on the complete catalytic cycle. Kinnunen used a B3LYP DFT method and characterized the same S_N2-like TS found by Griffin. However, Ivanova et al. attempted to overcome the high instability of the iodide leaving group in the gas phase by introducing NH_4^+ as a model of a counterion, considering the BP86 DFT method and including solvent effects "a posteriori" through the formalism of the PCM method.[26] These authors determined the geometry of two TS structures: one corresponded to the S_N2-like path, although it is strongly distorted compared with Griffin's and Kinnunen's structures; the other TS structure is related to a side-on attack, but in this case the I−CH_3−Rh angle is bent toward the two iodide ligands (Figure 1c). By including solvent effects, those authors found that the former TS is more stable, although the energy barrier was grossly overestimated. Very recently, Cheong et al.[27] made a further step by including the solvent effects in the calculations in a self-consistent manner at the BP86 DFT level. Surprisingly, the TS structure located in that study strongly differs from previous reported data, showing a rather long Me−I distance (5.2 Å) and a short Rh−Me bond (2.1 Å). These results do not agree with previous computational studies. Therefore, aiming to obtain a more accurate description of the MeI oxidative addition to rhodium complexes at the DFT level, this paper presents, for the first time, an unequivocal characterization of transition state structures in solution. Thus, TS structures were optimized in solution (methanol, dichloromethane) for the Monsanto system $[Rh(CO)_2I_2]^-$ and for models of neutral complexes, namely, *trans*-$[Rh(PEt_3)_2(CO)I]$ and $[Rh_2(\mu\text{-}Cl)_2(SPAN\text{-}PPh_2)(CO)_2]$, for which experimental data are available. Thermodynamic activation parameters calculated in the present study fully agree with experimental data.

Computational Details

All DFT calculations were carried out using the Amsterdam Density Functional (ADF2004.01) program developed by Baerends et al.[28] and vectorized by Ravenek.[29] The numerical integration scheme applied for the calculations was developed by te Velde et al.[30] The geometry optimization procedure was based on the method by Versluis and Ziegler.[31] Two DFT functionals were used in geometry optimization and frequency calculations: the local PBE exchange correlation potential combined with nonlocal exchange correction,[32] and the BP86 functional described as a combination between local VWN exchange−correlation potential with nonlocal Becke's exchange correction[33] and Perdew's correlation correction.[34]

(19) Freixa, Z.; Kamer, P. C. J.; Lutz, M.; Spek, A. L.; van Leeuwen, P. W. N. M. *Angew. Chem., Int. Ed.* **2005**, *44*, 4385.
(20) Griffin, T. R.; Cook, D. B.; Haynes, A.; Pearson, J. M.; Monti, D.; Morris, G. E. *J. Am. Chem. Soc.* **1996**, *118*, 3029.
(21) Cheong, M.; Schmid, R.; Ziegler, T. *Organometallics* **2000**, *19*, 1973.
(22) Ivanova, E. A.; Gisdakis, P.; Nasluzov, V. A.; Rubailo, A. V.; Rösch, N. *Organometallics* **2001**, *20*, 1161.
(23) Kinnunen, T.; Laasonen, K. *J. Mol. Struct. (THEOCHEM)* **2001**, *540*, 91.
(24) Kinnunen, T.; Laasonen, K. *J. Mol. Struct. (THEOCHEM)* **2001**, *542*, 273.
(25) Kinnunen, T.; Laasonen, K. *J. Organomet. Chem.* **2001**, *628*, 222.
(26) Amovili, C.; Barone, V.; Cammi, R.; Cances, E.; Cossi, M.; Mennuci, B.; Pomelli, C. S.; Tomasi, J. *Adv. Quantum. Chem.* **1999**, *32*, 227
(27) Cheong, M.; Ziegler, T. *Organometallics* **2005**, *24*, 3053.
(28) Baerends, E. J.; Ellis, D. E.; Ros, P. *Chem. Phys.* **1973**, *2*, 41. Baerends, E. J.; Ros, P. *Chem. Phys.* **1973**, *2*, 52
(29) Algorithms and Applications on Vector and Parallel Computers; te Riele, H. J. J., Deckker, T. J., van de Vorst, H. A., Eds.; Elsevier: Amsterdam, The Netherlands, 1987.
(30) Boerrigter, P. M.; te Velde, G.; Baerends, E. J. *Int. J. Quantum Chem.* **1988**, *33*, 87. te Velde, G.; Baerends, E. J. *J. Comput. Chem.* **1992**, *99*, 84
(31) Versluis, L.; Ziegler, T. *J. Chem. Phys.* **1988**, *88*, 322.
(32) Perdew, J. P.; Burke, K.; Ernzerhof, M. *Phys. Rev. Lett.* **1996**, *77*, 3875.

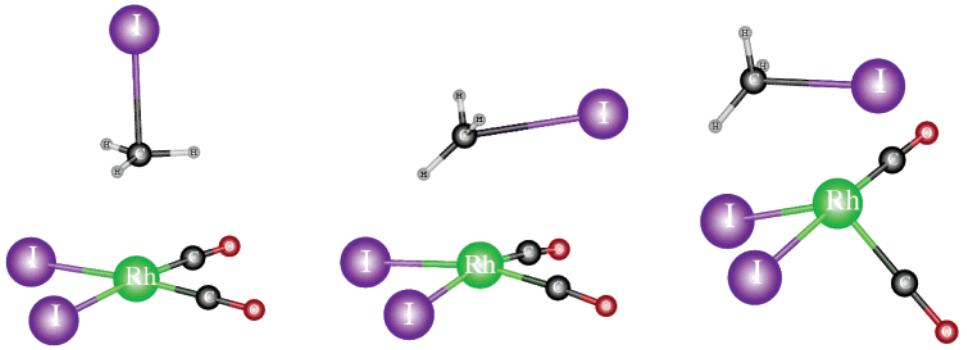

a ***b*** ***c***

Figure 1. Linear (***a***), bent (***b***), and front (***c***) transition state structures for nucleophilic attack by *cis*-$[Rh(CO)_2I_2]^-$ on methyl iodide.

Single-point calculations were performed with the hybrid B3LYP exchange and correlation functional.[35] Relativistic corrections were introduced by scalar-relativistic zero-order regular approximation (ZORA).[36] A triple-ξ plus two polarization Slater basis set was used for rhodium atoms, and plus one polarization function for the other atoms. For nonhydrogen atoms a relativistic frozen-core potential was used, including 3d for rhodium, 2p for phosphorus and chlorine, 4p for iodine, and 1s for carbon and oxygen. A numerical integration parameter of 5.0 was employed in optimization and single-point calculations. For frequencies computation, the integration criteria were increased to 6.0. Solvent effects were included variationally and in geometry optimization calculations by means of the conductor-like screening model (COSMO) of Klamt and Schüürmann[37] as implemented in ADF.[38] Methanol (dielectric constant $\epsilon_0 = 32.6$) and dichloromethane (dielectric constant $\epsilon_0 = 9.08$) were considered in order to fulfill the experimental conditions described for each case. Geometry convergence criteria were raised 1 order of magnitude up to 10^{-3} hartree·Å^{-1}. No symmetry constraints were used. Transition states were fully optimized and fully characterized by the presence of only one imaginary vibrational frequency. Mulliken[39] and VDD (Voronoi deformation density)[40] atomic population analyses were computed. The topological analysis of the electron density function was carried out using the Xaim program package.[41]

Results and Discussion

We considered the two reactants at infinite separation as the starting state. At the present level of theory, a prereaction complex was characterized, although it lies above the reactants by less than 0.5 kcal·mol^{-1}. Thus, activation energies were computed as the difference in energy between reactants and TS. Figure 1 displays the three types of TS structures that have been reported until now and that were characterized as true TSs at the present level of theory. Structure ***a*** corresponds to a S_N2-like approach characterized by a linear I−CH_3−Rh arrangement and by a I−CH_3−H angle close to 90°. The methyl hydrogen atoms are located in the equatorial plane of the five-coordinated carbon atom, which shows a trigonal bipyramidal geometry. This kind of structure has recently been characterized in a number of related cases,[42] and it was first proposed by Griffin et al.[20] In complex ***a***, the Rh−C and C−I distances agree with a concerted formation of the Rh−C bond and a rupture of the C−I bond. However, in structures ***b*** and ***c*** the iodine atom and the C−I bond approach the rhodium atom, although only structure ***c*** would correspond to a concerted three-center oxidative addition, i.e., simultaneous Rh−I and Rh−C formation and I−C breaking. Table 1 summarizes the main geometric parameters of the TS structures determined in the present study. The iodide−carbon bond length and the rhodium−carbon bond distances in the Monsanto TS structures fall in a narrow range in all cases, although the I−C bond in the *bent* structure is somewhat longer. Indeed, both I−C and Rh−C bonds (and Rh−I bond in the *front* structure) were characterized by the existence of bond critical points (bcp),[43] which were determined on the basis of the topological analysis of the electron density function. As expected, the value of the electron density at the bcp follows the same trend as the interatomic distances. In the *front* structure, the three-center nature of the TS is fully confirmed by the existence of the three bcp and the corresponding ring critical point (rcp).

In all three cases, vibrational analysis showed only one imaginary frequency which characterized unambiguously the stationary points as true TS structures. The values of the three frequencies vary in a narrow range despite the geometric differences. As found previously (vide supra), the most stable structure is the linear S_N2-like TS. However, geometric parameters optimized in this study including solvent effects differ substantially from the previously reported data. At the HF level

(33) Becke, A. D. *Phys. Rev. A* **1988**, *38*, 3098.
(34) Perdew, J. P. *Phys. Rev. B* **1986**, *34*, 7406. Perdew, J. P. *Phys. Rev. B* **1986**, *33*, 8822.
(35) Becke, A. D. *J. Chem. Phys.* **1993**, *98*, 564. Lee, C.; Yang, W.; Parr, R. G. *Phys. Rev. B* **1988**, *37*, 785. B3LYP optimizations have not been carried out because this option is not implemented yet in the ADF2004 program.
(36) (a) van Lenthe, E.; Baerends, E. J.; Snijders, J. G. *J. Chem. Phys.* **1993**, *99*, 4597. (b) van Lenthe, E.; Baerends, E. J.; Snijders, J. G. *J. Chem. Phys.* **1994**, *101*, 9783. (c) van Lenthe, J.; Ehlers, A.; Baerends, E. J. *J. Chem. Phys.* **1999**, *110*, 8943.
(37) Klamt, A.; Schüürmann, G. *J. Chem. Soc., Perkin Trans.* **1993**, *2*, 799.
(38) Pye, C. C.; Ziegler, T. *Theor. Chem. Acc.* **1999**, *191*, 396.
(39) Mulliken, R. S. *J. Chem. Phys.* **1955**, *23*, 1833.
(40) Fonseca Guerra, C.; Handgraaf, J.-W.; Baerends, E. J.; Bickelhaupt, F. M. *J. Comput. Chem.* **2004**, *25*, 189.
(41) Ortiz Alba, J. C.; Bo, C. *Xaim-1.0*; Universitat Rovira I Virgili: Tarragona, Spain. http://www.quimica.urv.es/XAIM.
(42) Bogdanov, B.; McMahon, T. B. *Int. J. Mass Spectrom.* **2005**, *241*, 205.
(43) According to the theory of atoms in molecules (AIM), the existence of a bond critical point (bcp) in the electron density distribution (in a fully optimized structure) is a necessary and sufficient condition for characterizing a chemical bond between two atoms. (a) Bader, R. F. W. *Atoms in Molecules: A Quantum Theory*; Oxford University Press: Oxford, UK, 1990. (b) Cortés-Guzmán, F.; Bader, R. F. W. *Coord. Chem. Rev.* **2005**, *249*, 633.

Table 1. Selected Geometrical Parameters, Mulliken and VDD Iodine Atomic Charges, TS Imaginary Frequency, and Activation Barriers of the Methyl Iodide Oxidative Addition on Rhodium Transition State Structures[a]

	d(I−C)	d(C−Rh)	d(Rh−I)	θ(I−C−Rh)	θ(I−C−H)	θ^{MULL}(I)	θ^{VDD}(I)	freq	$\Delta E^{\ddagger}$
$[Rh(CO)_2I_2(ICH_3)]^{-}$[b]									
linear (***a***)	2.592	2.577	5.167	176.7	91.8	−0.44	−0.45	323.26i	+7.66
bent (***b***)	2.775	2.641	3.803	89.2	144.2	−0.39	−0.38	386.05i	+38.31
					81.9				
front (***c***)	2.618	2.721	2.842	64.3	124.5	−0.01	−0.15	306.29i	+37.63
					95.5				
					86.7				
$[Rh(PH_3)_2(CO)I(ICH_3)]$[c]	2.585	2.594	5.178	177.3	92.1	−0.41	−0.43	339.01i	+6.80
$[Rh_2(\mu\text{-}Cl)_2(PH_3)_2(CO)_2(ICH_3)]$[c]	2.557	2.597	5.171	176.3	92.8	−0.40	−0.43	319.07i	+5.92

[a] Interatomic distances are in Å, angles in deg. Imaginary frequencies are expressed in cm^{-1} and activation barriers in $kcal \cdot mol^{-1}$. For comparison, optimized parameters for MeI were d(I−C) = 2.179 Å; d(C−H) = 1.091 Å, and θ(I−C−H) = 106.6°. [b] Geometries optimized in methanol. [c] Geometries optimized in dichloromethane.

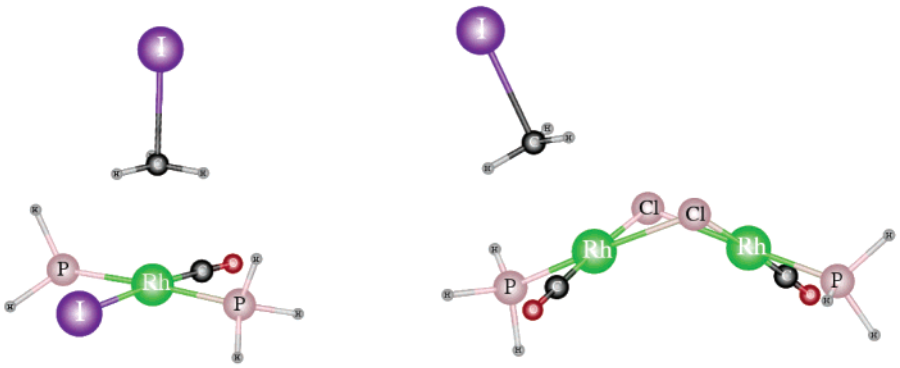

Figure 2. TS structures for MeI oxidative addition on *trans*-$[Rh(PH_3)_2(CO)I]$ (left) and to $[Rh_2(\mu\text{-}Cl)_2(PH_3)_2(CO)_2]$ (right) model complexes. See Table 1 for selected geometrical parameters.

and in the gas phase,[20] I−Me distances were found to be ca. 0.6 Å longer, and consequently, the Me−Rh distances were 0.4 Å shorter. The I−CH_3−Rh and CH_3−Rh−I_{plane} angles reported by Haynes showed higher distortion than our DFT-calculated results. B3LYP values in the gas phase[24] are closer to our values than to HF geometries, although in both gas-phase structures, the arrangement of the carbon methyl atom, especially the H−C−Rh angle being larger than 90°, suggests a product-like structure. All these differences can be explained by the lack of correlation effects in HF calculations, which are inadequate for describing metal−ligand bonds, and by the lack of solvent effects. It is worth mentioning that at the present DFT level TS geometry optimizations in the gas phase of the S_N2 TS structure ***a*** failed to converge, even when the Hessian matrix provided the desired eigenvector. In the TS, both the long Rh−I distances and the high negative charge developed on the iodine atom prevent the proper description of quasi *free* iodide in the gas phase. This effect is clearly reflected in the atomic charges of the iodine atom computed using two population analysis methods and collected in Table 1. Therefore, it was necessary to include solvent effects in order to obtain TS optimized structures, thus stabilizing the charge transfer toward the iodine atom. In a related case,[42] the same difficulty was recently overcome by considering explicitly solvated TS structures.

In the case of neutral phosphine complexes, we modeled the Cole−Hamilton system[6] by the *trans*-$[Rh(PH_3)_2(CO)I]$ compound and the new dimeric $[Rh_2(\mu\text{-}Cl)_2$(SPAN-$PPh_2)(CO)_2]$ catalyst reported by Freixa et al.[19] by the complex $[Rh_2(\mu\text{-}Cl)_2(PH_3)_2(CO)_2]$. In the latter case, oxidative addition on only one of the rhodium centers has been considered, according to experimental results.[19] In both cases, we characterized the linear S_N2-like transition state as is shown in Table 1 and Figure 2, which displays the molecular structures of those TSs.

Table 2. Values of the Electron Density (in electons·bohr^{-1}) at the Bond Critical Points (3,−1) for Each I-CH_3-Rh TS's Moiety

	I−C	C−Rh	Rh−I
CH_3I	0.103		
$[Rh(CO)_2I_2(ICH_3)]^{-}$			
linear (***a***)	0.047	0.042	
bent (***b***)	0.035	0.042	
front (***c***)[a]	0.046	0.032	0.047
$[Rh(PH_3)_2(CO)I(ICH_3)]$	0.048	0.041	
$[Rh_2(\mu\text{-}Cl)_2(PH_3)_2(CO)_2(ICH_3)]$	0.049	0.040	

[a] For this structure, a ring critical point (3,+1) was characterized (ρ(rcp) = 0.028).

Regarding the methyl iodide moiety, no large differences were found between the Monsanto TS structure and those found for phosphine-substituted neutral complexes. The distances I−CH_3 and CH_3−Rh and I−CH_3−H angles were very similar, as well as the imaginary vibrational frequencies (see Table 1). The I−CH_3 bond distances followed a clear trend, $[Rh_2(\mu\text{-}Cl)_2(PH_3)_2(CO)_2]$ < *trans*-$[Rh(PH_3)_2(CO)I]$ < Monsanto, as do the values of the electronic density at the bcp (Table 2). It is interesting to note that the lowest barrier that we obtained corresponds to the fastest catalyst, i.e., to the rhodium dimer. Indeed, energy barriers followed the same trend displayed by the I−CH_3 bond distance in the TSs.

Table 3. Calculated Activation Parameters in MeI Oxidative Addition Reaction on Mono- and Dirhodium Catalysts[a]

	$\Delta S^{\ddagger}$	$\Delta E^{\ddagger}$	$\Delta H^{\ddagger}$	$\Delta G^{\ddagger}$
cis-$[Rh(CO)_2I_2]^-$[b]				
exp [ref 20]	−28.7		14.3	22.9
calc (PBE)		6.7		
calc (BP86)[c]	−36.9	7.7	8.2	19.2
calc (BP86)[d]	−31.8	7.7	8.2	17.7
calc (B3LYP)		13.7	14.2 [e]	24.7[f]
calc (B3LYP) (***a***)[g]		16.3		20.8
calc (B3LYP) (***a***)[g]		13.0		16.9
calc (MP2) (***a***)[h]		17.0		
calc (MP2) bent (***b***)[h]		60.9		
calc (BP86) bent-2[c,i]	−43.9		13.8	26.9
calc (BP86) front (***c***)[j]		31.6		47.0
calc (BP86) back[j]		34.9		32.2
trans-$[Rh(PEt_3)_2(CO)I]$				
exp [ref 6]	−26.8		13.4	21.3
trans-$[Rh(PH_3)_2(CO)I]$[k]				
calc (BP86)[c]	−37.1	6.8	7.6	18.7
calc (B3LYP)		12.7	13.5[e]	23.7[f]
$[Rh_2(\mu\text{-}Cl)_2(SPAN{-}PPh_2)_2(CO)_2]$				
exp [ref 19]	−39.1		7.7	19.4
$[Rh_2(\mu\text{-}Cl)_2(PH_3)_2(CO)_2]$[k]				
calc (BP86)[c]	−41.5	5.9	7.0	19.4
calc (B3LYP)		11.1	12.2[e]	23.5[f]
$[Rh_2(\mu\text{-}Cl)_2(PMe_3)_2(CO)_2]$[k]				
calc (BP86)		5.5		
calc (B3LYP)		10.4		

[a] At 298.15 K and 1 atm. All energies are in kcal·mol^{-1}, entropies in cal·K^{-1}·mol^{-1}. [b] Solvent methanol ($\epsilon_0 = 32.6$). [c] $\Delta G_{solv}^{\ddagger} = \Delta H_{solv}^{\ddagger} - T\Delta S_{solv}^{\ddagger}$. [d] $\Delta G_{solv}^{\ddagger} = \Delta H_{solv}^{\ddagger} - T\Delta S_{gas}^{\ddagger}$. [e] Value estimated as $\Delta H_{solv}^{\ddagger}(B3LYP) = \Delta H_{solv}^{\ddagger}(BP86)_{corr} + \Delta E_{solv}^{\ddagger}(B3LYP)$, where $\Delta H_{solv}^{\ddagger}(BP86)_{corr}$ is the difference between $\Delta H_{solv}^{\ddagger}$ (BP86) − $\Delta E_{solv}^{\ddagger}$(BP86). [f] $\Delta G_{solv}^{\ddagger}(B3LYP) = \Delta H_{solv}^{\ddagger}(B3LYP) - T\Delta S_{solv}^{\ddagger}$(BP86). [g] The $\Delta E^{\ddagger}$ and $\Delta G^{\ddagger}$ results reported by Laasonen for both structures include zero-point corrections, ref 24. [h] MP2 single-point calculated energies from optimized RHF/LANL2DZ structures, ref 20. [i] Optimized BP86 energies reported by Cheong. Transition state geometry corresponds to the one labeled as TS[1−2] in original paper, ref 27. [j] The *front* transition state corresponds to TS(A1B3-front) labeled in the original paper and *back* to the *cis*-$[Rh(CO)_2I_2]^-[NH_4]^+$ neutral species (TS(A1B3-front)), ref 22. [k] Solvent dichloromethane ($\epsilon_0 = 9.08$).

Thermochemical data obtained from kinetic measurements are available for the Monsanto, for *trans*-$[Rh(PEt_3)_2(CO)I]$, and for $[Rh_2(\mu\text{-}Cl)_2(SPAN\text{-}PPh_2)(CO)_2]$ catalysts. Therefore, we sought to calculate activation free energies and activation entropies by including standard corrections to the energy barriers, and to compare those with experimental and previously computed data. Although contributions arising from the changes in the internal degrees of freedom when going from reactants to the transition state are included in the standard statistical corrections applied here, changes in the solvent part are not accounted for.[44] Solvation energies computed in the framework of continuum solvent models, such as COSMO used in our calculations,[38] have been considered as an electrostatic contribution to enthalpy,[27] so we followed the same assumption. Zero-point energy, internal energy, and entropic contributions were computed considering the solvent in the calculation of the harmonic frequencies. Gas-phase entropy was obtained by recalculating the frequencies.

Table 3 collects several values computed in this study and those reported by other authors for comparison. We computed the energy barrier by using different functionals (PBE, BP86) and by performing single-point B3LYP calculations on the geometry optimized at the BP86 level. Values computed for MeI oxidative addition on the Monsanto *cis*-$[Rh(CO)_2I_2]^-$ catalyst using pure DFT functionals correspond to the lowest values computed until now (6.7 and 7.7 kcal·mol^{-1}), whereas the value obtained using the hybrid B3LYP functional is more in accordance with the experiment and almost coincides with a value reported by Laasonen.[24] As mentioned before, previous studies overestimated the energy barrier. The agreement between the activation enthalpy estimated at the B3LYP level and the experimental value is excellent. In the most recent report, Cheong[27] found a good agreement between calculated and experimental activation enthalpies (13.8 vs 14.3 kcal·mol^{-1}), although the geometry of the reported transition state differs substantially from the linear S_N2 structure characterized by us and others. Moreover, the $\Delta S_{MeOH}^{\ddagger}$ value calculated in this study at the same level of calculation is also in good agreement with experimental results and lower than previously reported data. In this context, the $\Delta S_{gas}^{\ddagger}$ parameter, computed from a calculation of the vibrational frequencies in the gas phase, is closer to the experimental result than the value computed in solution. It should be noticed that, in any case, the discrepancies are small.

The results for the Cole−Hamilton catalyst model *trans*-$[Rh(PH_3)_2(CO)I]$ show that the BP86-calculated activation enthalpy is 5.8 kcal·mol^{-1} lower than the experimental value, whereas the B3LYP-estimated enthalpy reproduces the experimental data fairly well. The activation entropy value is also overestimated, although within the experimental error. Our estimation of the activation free energy at the B3LYP calculations reproduces the experimental measure. Computed activation parameters are thus in full agreement with experiment, which indicates that phosphine-rhodium compounds provide faster catalysts than the Monsanto one. Recently, Freixa et al.[19] have shown that the highest activities (when using phosphine ligands) for oxidative addition of MeI to rhodium are obtained when using dinuclear compounds containing SPANphos as bridging diphosphine. The optimized activation parameter for the model system $[Rh_2(\mu\text{-}Cl)_2(PH_3)_2(CO)_2]$ calculated at the BP86 level was 5.9 kcal·mol^{-1}, which corresponds to a lower activation barrier than that computed for mononuclear catalysts. Entropy and enthalpy at BP86 values show a good agreement with experimental values. In this case, B3LYP single-point calculations overestimate the activation enthalpy by 4.5 kcal·mol^{-1}. As Table 2 shows, the B3LYP-calculated free activation energy is overestimated in this case, while the BP86 functional shows a nice agreement with experimental data. To check if the activation barrier would decrease further by increasing the electron density at the rhodium center, PH_3 ligands were replaced by PMe_3 as a model for better donor ligands.[45] Indeed, the activation energy for MeI oxidative addition on $[Rh_2(\mu\text{-}Cl)_2(PMe_3)_2(CO)_2]$ compounds was the lowest barrier found in this work (see Table 3), and the I−CH_3 distance was the shortest (2.539 Å).

(44) Wood, R. H.; Yezdimer, E. M.; Sakane, S.; Barriocanal, J. A.; Doren, D. J. *J. Chem. Phys.* **1999**, *110*, 1329.

(45) (a) Gonzalez-Banco, O.; Branchadell, V. *Organometallics* **1997**, *16*, 5556−5562. (b) Woska, D.; Prock, A.; Giering, W. P. *Organometallics* **2000**, *19*, 4629−4638. (c) Haberlen, O.; Rosch, N. *J. Phys. Chem.* **1993**, *97*, 4970−4073.

Conclusions

From the results and analysis presented above, we can draw the following conclusions.

(i) The transition state for the oxidative addition of MeI on square planar rhodium complexes corresponds to a S_N2 nucleophilic attack by the metal compound on methyl iodide. The geometry of the TS structure shows a collinear I−C−Rh disposition. A concerted three-center TS structure exists as well, although it lies at high energy.

(ii) Activation enthalpies and activation entropies calculated in this study including solvent effects were in excellent agreement with experimental values. For mononuclear complexes, the B3LYP functional provided results superior to other DFT methods. However, for binuclear complexes, the hybrid functional overestimated the barrier, whereas the BP86 functional did not.

(iii) The nucleophilic character of the rhodium atom, tuned by introducing electron donor ligands such as phosphines, greatly influences the barrier. Indeed, the more nucleophilic the rhodium center is, the lower the barrier is. This experimental observation perfectly correlates with the results obtained in the present study. Geometrical parameters of the TS structures also showed that when the nucleophilic character of the metal center increases, the C−I distance decreases, and therefore an earlier TS is obtained.

(iv) Finally, the results of the DFT calculations including solvent effects showed that dirhodium complexes coordinated to monophosphines are the most active catalysts reported until now and are in perfect agreement with experimental findings. Further studies on the complete reaction cycle for diphosphine bimetallic catalysts are in progress.

Acknowledgment. The authors are indebted to the ICIQ Foundation for financial support. M.F. thanks the Torres Quevedo program of the MEC of Spain. Z.F. is pleased to acknowledge the Ramon y Cajal program of the MEC for financial support. We thank Mr. Joan Iglesias for his technical expertise.

Supporting Information Available: Cartesian coordinates (in Å) of the structures considered in this study. This material is available free of charge via the Internet at http://pubs.acs.org.

OM050554G